IOP Publishing Journal of Physics G: Nuclear and Particle Physics

J. Phys. G: Nucl. Part. Phys. **43** (2016) 095107 (18pp) doi:10.1088/0954-3899/43/9/095107

New type of chiral motion in even–even nuclei: the ^{138}Nd case

A A Raduta[1,2,4], Al H Raduta[1] and C M Petrache[3]

[1] Department of Theoretical Physics, Institute of Physics and Nuclear Engineering, Bucharest, PO Box MG6, Romania
[2] Academy of Romanian Scientists, 54 Splaiul Independentei, Bucharest 050094, Romania
[3] Centre de Spectrométrie de Masse, Université Paris-Sud and CNRS/IN2P3, Bâtiment 104-108, F-91405 Orsay, France

E-mail: raduta@nipne.ro

Received 22 April 2016, revised 24 June 2016
Accepted for publication 28 June 2016
Published 18 August 2016

Abstract

The phenomenological generalized coherent state model Hamiltonian is amended with a many body term describing a set of nucleons moving in a shell model mean-field and interacting among themselves with pairing, as well as with a particle–core interaction of spin–spin type. The model Hamiltonian is treated in a restricted space consisting of the core projected states associated to the band ground, β, γ, $\widetilde{\gamma}$, 1^+ and $\widetilde{1}^+$ and two proton aligned quasiparticles coupled to the states of the collective dipole band. The chirally transformed particle–core states are also included. The Hamiltonian contains two terms which are not invariant to the chiral transformations relating the right-handed frame ($\mathbf{J_F}$, $\mathbf{J_p}$, $\mathbf{J_n}$) and the left-handed ones ($-\mathbf{J_F}$, $\mathbf{J_p}$, $\mathbf{J_n}$), ($\mathbf{J_F}$, $-\mathbf{J_p}$, $\mathbf{J_n}$), ($\mathbf{J_F}$, $\mathbf{J_p}$, $-\mathbf{J_n}$) where $\mathbf{J_F}$, $\mathbf{J_p}$, $\mathbf{J_n}$ are the angular momenta carried by fermions, proton and neutron bosons, respectively. The energies defined with the particle–core states form four bands, two of them being degenerate in the present formalism, while the other two exhibit chiral properties reflected by energies, electromagnetic properties and the energy staggering function. A numerical application for ^{138}Nd shows a good agreement between results and the corresponding experimental data.

Keywords: chiral phenomenon, chiral symmetry, chiral doublet bands, M1 and E2 transition rates

(Some figures may appear in colour only in the online journal)

[4] Author to whom any correspondence should be addressed.

1. Introduction

Many nuclear properties are explored through the interaction with an electromagnetic field. The electric and magnetic components of the field are used to unveil some properties of an electric and magnetic nature, respectively. Good examples along this line are the scissor-like states [1–3] and spin–flip excitations [4], which have been widely treated by various groups. The scissor mode is associated to the angular oscillation of the proton against the neutron system with a total strength proportional to the nuclear deformation squared, which confirms the collective character of the excitation [3, 4].

Due to this feature it was believed that the magnetic collective properties, in general, show up in deformed systems. However, this is not supported experimentally, since there are magnetic dipole bands that have been observed often in almost spherical nuclei. Indeed, there exists experimental evidence for magnetic bands in nearly spherical nuclei where the ratio between the moment of inertia and the $B(E2)$ value for exciting the first 2^+ from the 0^+ ground state, $\mathcal{I}^{(2)}/B(E2)$, takes large values, of the order of 100 $(\text{eb})^{-2}$ MeV^{-1} [5]. These large values can be consistently explained by large transverse magnetic dipole moments, which induce dipole magnetic transitions but negligible charge quadrupole moments [5]. Indeed, there are several experimental data sets showing that the dipole bands have large values for $B(M1) \sim 1 - 3\mu_N^2$, and very small values of $B(E2) \sim 0.1(\text{eb})^2$ (see for example [6]). The states are different from the scissor-like ones, exhibiting instead a shear character. A system with a large transverse magnetic dipole moment may also consist of a triaxial core to which a proton particle and a neutron hole are coupled. The maximal transverse dipole momentum is achieved when, for example, $\mathbf{j_p}$ is oriented along the short axis of the core and $\mathbf{j_n}$ along the long axis of the core, which rotates around the intermediate axis. Suppose that the three orthogonal angular momenta form a right-handed frame. If the Hamiltonian describing the interacting system of protons, neutrons and the triaxial core is invariant to the transformation which changes the orientation of one of the three angular momenta, i.e. the right-handed reference frame is transformed to a left-handed one, the system exhibits chiral symmetry. As always happens, such a symmetry is identified when it is broken and consequently for the two reference frames the system acquires distinct energies, otherwise close to each other. Thus, a signature for a chiral symmetry characterizing a triaxial system is the existence of two $\Delta I = 1$ bands which are close in energy. Experimentalists identified some other fingerprints for the existence of chiral doublets including the one already mentioned. These refer to the electromagnetic intra- and inter-band transitions as well as the behavior of the energy staggering function which should be similar for the two bands. The energy staggering has to be almost constant and exhibit close values in the two bands. The chiral doublet bands show up in the laboratory frame where the chiral symmetry is restored.

In [7, 8] we attempted to investigate another chiral system consisting of one phenomenological core with two components, one for protons and one for neutrons, and two quasiparticles whose total angular momentum $\mathbf{J_F}$ is oriented along the symmetry axis of the core, due to the particle–core interaction. In the quoted references we proved that states of total angular momentum $\mathbf{I}$, where the three components mentioned above carry the angular momenta $\mathbf{J_p}$, $\mathbf{J_n}$, $\mathbf{J_F}$ which are mutually orthogonal, do exist. Such a configuration seems to be optimal for defining a large transverse magnetic moment that induces large M1 transitions. In choosing the candidate nuclei with chiral features, we were guided by the suggestion [5] that triaxial nuclei may favor orthogonality of the aforementioned three angular momenta and therefore may exhibit a large transverse magnetic moment. In the previous publications, the formalism was applied to ^{192}Pt, ^{188}Os and ^{190}Os, which satisfy the triaxiality signature condition [7, 8].

Here we simplify the Hamiltonian used in the previous publications by keeping from the particle–core interaction only the spin–spin term. The model Hamiltonian is treated in a restricted space consisting of the angular momentum projected states of the core describing six collective bands and of a subspace of states spanned by two quasiparticles with the total angular momentum J aligned along the symmetry axis, which are coupled with the states of the collective dipole band to a total angular momentum larger or equal to I. The chiral properties are studied with the $2qp \otimes$ core dipole states and their chiral transformed states. The formalism is applied to ^{138}Nd, for which some relevant data are available [23, 24].

The work sketched above is developed according to the following plan. In section 2 we briefly present the main ingredients of the generalized coherent state model (GCSM) which was used to describe the states of the core. The Hamiltonian describing the particle–core interaction is presented in section 3. The chiral features of the particle–core Hamiltonian are evidenced in section 4. Numerical results for the specific case of ^{138}Nd are discussed in section 5, while section 6 is devoted to the final conclusions.

2. Brief review of the GCSM

The nuclear system to be described consists of a set of pairing correlated nucleons moving in a high j-shell and interacting with a collective core. The core is described by the generalized coherent state model (GCSM) [12], which is an extension of the coherent state model (CSM) [13] to a heterogeneous system of protons and neutrons. The aim of this extension was also to describe the magnetic-collective dipole bands of scissor type. Since one deals with two quadrupole bosons, $b^{\dagger}_{p,\mu}$ and $b^{\dagger}_{n,\mu}$, instead of one, one expects to have a more flexible model and to find a simpler solution satisfying the restrictions required by CSM. Essentially, GCSM defines first a restricted collective space following a set of criteria formulated in [13], and an effective boson Hamiltonian. The restricted collective space is spanned by a boson state basis obtained by projecting out the components of good angular momentum from a set of orthogonal deformed states. Due to their specific properties, these define the model states for six bands: ground, β, γ, $\widetilde{\gamma}$, 1^+ and $\widetilde{1^+}$. Their analytical expressions are

$$\begin{aligned}
&|g;\, JM\rangle = N^{(g)}_J P^J_{M0}\psi_g, \quad |\beta;\, JM\rangle = N^{(\beta)}_J P^J_{M0}\Omega_\beta\psi_g, \quad |\gamma;\, JM\rangle \\
&\qquad = N^{(\gamma)}_J P^J_{M2}(\Omega^{\dagger}_{\gamma,p,2} + \Omega^{\dagger}_{\gamma,n,2})\psi_g, \\
&|\widetilde{\gamma};\, JM\rangle = N^{(\widetilde{\gamma})}_J P^J_{M2}(b^{\dagger}_{n2} - b^{\dagger}_{p2})\psi_g,\ |1;\, JM\rangle = N^{(1)}_J P^J_{M1}(b^{\dagger}_n b^{\dagger}_p)_{11}\psi_g, \\
&|\tilde{1};\, JM\rangle = N^{(\tilde{1})}_J P^J_{M1}(b^{\dagger}_{n1} - b^{\dagger}_{p1})\Omega^{\dagger}_\beta\psi_g,\ \psi_g = \exp\left[(d_p b^{\dagger}_{p0} + d_n b^{\dagger}_{n0}) - (d_p b_{p0} + d_n b_{n0})\right]|0\rangle.
\end{aligned} \tag{2.1}$$

Here, the following notations have been used

$$\begin{aligned}
&\Omega^{\dagger}_{\gamma,k,2} = (b^{\dagger}_k b^{\dagger}_k)_{22} + d_k\sqrt{\frac{2}{7}}\,b^{\dagger}_{k2}, \quad \Omega^{\dagger}_k = (b^{\dagger}_k b^{\dagger}_k)_0 - \sqrt{\frac{1}{5}}\,d^2_k, \quad k = p,\, n, \\
&\Omega^{\dagger}_\beta = \Omega^{\dagger}_p + \Omega^{\dagger}_n - 2\Omega^{\dagger}_{pn}, \quad \Omega^{\dagger}_{pn} = (b^{\dagger}_p b^{\dagger}_n)_0 - \sqrt{\frac{1}{5}}\,d^2_p, \\
&\hat{N}_{pn} = \sum_m b^{\dagger}_{pm} b_{nm}, \quad \hat{N}_{np} = (\hat{N}_{pn})^{\dagger}, \quad \hat{N}_k = \sum_m b^{\dagger}_{km} b_{km}, \quad k = p,\, n.
\end{aligned} \tag{2.2}$$

$N^{(k)}_J$ with $k = g,\ \beta,\ \gamma,\ \widetilde{\gamma}, 1\ ,\ \tilde{1}$ are normalization factors, while P^J_{MK} stands for the angular momentum projection operator. Note that for the gamma band there are two candidates which satisfy the requirements of the CSM. One function is symmetric, while the other one is

asymmetric with respect to the proton–neutron permutation. In [9, 12] we alternatively used the two versions for the gamma band and we found that for some nuclei the fitting procedure yielded a better description of the data both for energies and $B(E2)$ values, when the choice of the asymmetric function was made. In [16] it was proved that the asymmetric gamma states can be excited from the ground state by the asymmetric component of the electric quadrupole transition operator. The possibility of having two distinct phases for the collective motion in the gamma band has also been considered in [22] within a different formalism. We do not claim, however, that this is a general feature for the gamma band, but that for some nuclei the properties specific for asymmetric state may prevail over those characterizing the symmetric gamma states. On the other hand, some experimental results like those obtained from (α, α') scattering support the isoscalar structure of the gamma-band states although even this result is not proved to be true in general. For this reason, we choose here the option of symmetric gamma states which, indeed, provides a better description of the data for the case of ^{138}Nd considered here.

Following the CSM criteria, for the dipole bands we also have two candidate functions, $|1, JM\rangle$ and $|\tilde{1}; JM\rangle$. In [9] the asymptotic behavior of both states has been considered in the intrinsic reference frame. The important results which came out are: (a) the first state is a generalization of the wave functions used by the two rotor [1] and two liquid drops [21] models; (b) the first state corresponds to a lower excitation energy than the second state. These two properties induced us to use $|1, JM\rangle$ as model states for the dipole bands studied in the present work.

So far, all reported calculations considered equal deformations for protons and neutrons

$$\rho = \sqrt{2}\, d_p = \sqrt{2}\, d_n \equiv \sqrt{2}\, d. \tag{2.3}$$

The projected states defined by equation (2.1) describe the essential nuclear properties in the limiting cases the spherical and well deformed systems. Details about the relevant properties of the angular momentum projected states may be found in [12]. Written in the intrinsic reference frame, the projected states are combinations of different K components. The dominant components of the function superpositions have $K = 0$ for the ground and beta bands, $K = 2$ for the gamma bands, and $K = 1$ for the dipole bands. Actually this feature represents a strong support for the band assignments to the model projected states.

According to the salient features of the projected states basis [12], it is desirable to find a boson Hamiltonian which is effective in that basis, i.e. to be quasi-diagonal. It is constructed with the rotation invariants of lowest order and limited to the fourth order in bosons. Since the basis contains both symmetric and asymmetric states with respect to the proton–neutron (p–n) permutation, the effective Hamiltonian should be symmetric with respect to the p–n permutation.

Therefore, we seek an effective Hamiltonian for which the projected states (2.1) are, at least in a good approximation, eigenstates in the restricted collective space. The simplest Hamiltonian fulfilling this condition is

$$\begin{aligned} H_{\rm GCSM} = {} & A_1 (\hat{N}_p + \hat{N}_n) + A_2 (\hat{N}_{pn} + \hat{N}_{np}) + \frac{\sqrt{5}}{2}(A_1 + A_2)(\Omega^\dagger_{pn} + \Omega_{np}) \\ & + A_3 (\Omega^\dagger_p \Omega_n + \Omega^\dagger_n \Omega_p - 2\Omega^\dagger_{pn}\Omega_{np}) + A_4 \hat{J}^2, \end{aligned} \tag{2.4}$$

with $\hat{J}$ denoting the proton and neutron total angular momentum. The Hamiltonian given by equation (2.4) has only one off-diagonal matrix element in the basis (2.1), that is $\langle\beta; JM|H_{\rm GCSM}|\tilde{\gamma}; JM\rangle$. However, our calculations show that this affects the energies of the β and $\tilde{\gamma}$ bands by only a few keV. Therefore, the excitation energies of the six bands are in a

good approximation, given by the diagonal element

$$E_J^{(k)} = \langle k; JM|H_{\rm GCSM}|k; JM\rangle - \langle g; 00|H_{\rm GCSM}|g; 00\rangle, \quad k = g, \beta, \gamma, 1, \tilde{\gamma}, \tilde{1}. \tag{2.5}$$

The analytical behavior of the energies and wave functions in the extreme limits of vibrational and rotational regimes have been studied in [12, 14–20].

It is worth mentioning that the proposed phenomenological boson Hamiltonian has a microscopic counterpart obtained through the boson expansion procedure from a many body Hamiltonian for a proton and neutron interacting system. In this case the structure coefficients A_1, A_2, A_3, A_4 are analytically expressed in terms of the one- and two-body interactions matrix elements. A detailed review of the results obtained with the CSM and GCSM is presented in the recently published book of one of the present authors [25].

We note that $H_{\rm GCSM}$ comprises a term which is not invariant to the change of the sign of either $\mathbf{J}_p$ or $\mathbf{J}_n$. For what follows it is useful to write $H_{\rm GCSM}$ in the form

$$H_{\rm GCSM} = H'_{\rm GCSM} + 2A_4\mathbf{J}_p \cdot \mathbf{J}_n. \tag{2.6}$$

3. Extension to a particle–core system

The particle–core interacting system is described by the following Hamiltonian

$$H = H_{\rm GCSM} + \sum_\alpha \epsilon_a c_\alpha^\dagger c_\alpha - \frac{G}{4}P^\dagger P - X_{sS}\mathbf{J_F}\cdot\mathbf{J_c}. \tag{3.1}$$

The core is described by $H_{\rm GCSM}$, while the particle system is described by the next two terms standing for a spherical shell model mean-field and pairing interaction of the alike nucleons, respectively. The notation $|\alpha\rangle = |nljm\rangle = |a, m\rangle$ is used for the spherical shell model states. The particles interact with the core through a spin–spin force with the strength denoted by X_{sS}. The angular momenta carried by the core and particles are denoted by $\mathbf{J_c}(=\mathbf{J_p} + \mathbf{J_n})$ and $\mathbf{J_F}$, respectively.

The mean field plus the pairing term is quasi-diagonalized by means of the Bogoliubov–Valatin transformation. The free quasiparticle term is $\sum_\alpha E_a a_\alpha^\dagger a_\alpha$ where the quasiparticle creation (annihilation) operators are denoted by $a_{jm}^\dagger$ (a_{jm}), while E_a stands for the quasiparticle energy. We restrict the single-particle space to a proton single-j state. In the space of the particle–core states we, therefore, consider the states

$$\begin{aligned}
&|BCS\rangle \otimes |1; JM\rangle,\\
&\Psi_{JI;M}^{(2qp;J1)} = N_{JI}^{(2qp;J1)} P^I_{M\,(J+1)}\,(a_j^\dagger a_j^\dagger)_{JJ}|BCS\rangle \otimes (b_n^\dagger b_p^\dagger)_{11}\psi_g\\
&\quad = N_{JI}^{(2qp;J1)} \sum_{J'=\text{even}} C^{J\ J'\ I}_{J\ 1\ J+1}(N^{(1)}_{J'})^{-1}[(a_j^\dagger a_j^\dagger)_J|BCS\rangle \otimes |1; J'\rangle]_{IM}.
\end{aligned} \tag{3.2}$$

where $|BCS\rangle$ is the quasiparticle vacuum and $N_{JI}^{(2qp;J1)}$ are the projected state norms.

Why are these bases states favored in describing the chiral properties of some nuclei? The answer to this question was given in [7, 8], where it was shown that for low spin the angular momenta corresponding to the satellite nucleons and proton and neutron cores are mutually orthogonal, which assures a large transversal magnetic dipole moment; this geometry is optimal for inducing large M1 transition rates. Intuitively, this can be understood due to the following arguments. In the intrinsic frame the unprojected state has $K = 1$. This means that the angular momenta carried by the proton and the neutron bosons are almost perpendicular to the symmetry axis. In other words in the lowest projected state, $J = 1$, the angular momenta carried by the proton- and neutron-bosons are almost anti-aligned. With

increasing the rotation frequency, the two angular momenta will align with each other above a critical frequency. On the path to this final regime the angle between the two angular momenta unavoidably passes through the value $\pi/2$. On the other hand the angular momentum of the two quasiparticle factor states is oriented along the symmetry axis since the state is characterized by a maximal K. The question arises: to what extent is the hypothesis of oblate like orbits for the two quasiparticles coupled to the core realistic or not? To answer this question we invoke some known features, valid in specific regions of the nuclear chart, like that corresponding to ^{138}Nd. It is known that in the nuclei of the $A = 130$–140 mass region, which are γ-soft, the valence protons occupy the lower half of the $h_{11/2}$ orbital driving the nucleus to a prolate shape ($\gamma \sim 0^{\circ}$), while the valence neutrons occupy the upper half of the $h_{11/2}$ orbital, which favors an oblate shape ($\gamma \sim 60^{\circ}$). One expects, therefore, coexisting prolate and oblate minima for the potential energy. For nuclei with $Z \sim 60$ the $h_{11/2}[505]9/2$ and $h_{11/2}[505]11/2$ orbitals are strongly down sloping in energy on the oblate side ($\varepsilon_2 < 0$ of the Nilsson diagram) and may also contribute to the stability of the oblate shape. Indeed, collective oblate bands built on or involving these single high-Ω $h_{11/2}$ orbitals have been observed to low spin ($11/2^{-}$) in light iodine nuclei [10] and at medium spins in ^{136}Ce (see [11] and references therein).

In conclusion, this basis is optimal for describing a composite system which rotates around an axis not situated in any of the principal planes of the density distribution ellipsoid. In the space of angular momenta, in the case of the three orthogonal spins one may interpret them as a reference frame, denoted by F_1. Suppose that F_1 has a right-handed character.

We note that the Hamiltonian H is not invariant to the chiral transformations, defined by changing the sign of one of the angular momenta $\mathbf{J_F}$, $\mathbf{J_p}$ and $\mathbf{J_n}$. Also, H is not invariant to any rotation generated by the components of the mentioned three angular momenta. It is however invariant to the rotations generated by the total angular momentum. It is worthwhile to write H as a sum of a chiral invariant term H' and the non-invariant terms

$$H = H' + \sum_{\alpha} E_a a_{\alpha}^{\dagger} a_{\alpha} + 2A_4 \mathbf{J_p} \cdot \mathbf{J_n} - X_{sS} \mathbf{J_F} \cdot \mathbf{J_c}. \tag{3.3}$$

Let us denote by C_{12} the chiral transformation which changes the sign of $\mathbf{J_F}$. Applying this transformation to the frame F_1 one obtains a new frame denoted by F_2. Similarity, by changing the sign of $\mathbf{J_p}$, the frame F_1 goes to F_3, while by changing $\mathbf{J_n} \rightarrow -\mathbf{J_n}$, the newly obtained frame is denoted by F_4. The non-invariance of H against chiral transformations requires the extension of the basis (3.2) by adding the chiral transformed states: $C_{12}\Psi^{(2qp;J1)}_{JI;M}$, $C_{13}\Psi^{(2qp;J1)}_{JI;M}$, $C_4\Psi^{(2qp;J1)}_{JI;M}$. In what follows we shall study the spectrum of H in the extended basis

$$\begin{aligned} &|BCS\rangle \otimes |1; JM\rangle; \quad C_{12}|BCS\rangle \otimes |1; JM\rangle; \quad C_{13}|BCS\rangle \otimes |1; JM\rangle; \quad C_{14}|BCS\rangle \otimes |1; JM\rangle \\ &\Psi^{(2qp;J1)}_{JI;M}; \quad C_{12}\Psi^{(2qp;J1)}_{JI;M}; \quad C_{13}\Psi^{(2qp;J1)}_{JI;M}; \quad C_{14}\Psi^{(2qp;J1)}_{JI;M}. \end{aligned} \tag{3.4}$$

4. Chiral bands

The expectation values of the model Hamiltonian for the particle–core system, for a given member state from the basis and alternatively for its chiral transformed state, lead to two sets of energies defining two independent bands exhibiting the properties of a chiral doublet.

To prove this statement we consider for example the pair of states $\Psi^{(2qp;J1)}_{JI;M}$ and $C_{12}\Psi^{(2qp;J1)}_{JI;M}$. The transformation C_{12} does not commute with H due to the presence of the

spin–spin term, but it anti-commutes with the spin–spin term

$$\{-X_{sS}\mathbf{J_F}\cdot\mathbf{J_c},\, C_{12}\}=0. \tag{3.5}$$

If $|\psi\rangle$ is an eigenstate of $-X_{sS}\mathbf{J_F}\cdot\mathbf{J_c}$ corresponding to the eigenvalue λ, then the transformed function $C_{12}|\psi\rangle$ is also eigenfunction corresponding to the eigenvalue $-\lambda$. One eigenfunction of the spin–spin interaction is $\Psi^{(2qp;J1)}_{JI;M}$ with the eigenvalue

$$\lambda_{JI}=-X_{sS}\,(N^{(2qp;J1)}_{JI})^2\sum_{J'}(C^{J\ J'\ I}_{J\ 1\ J+1})^2\,(N^{(1)}_{J'})^{-2}[I\,(I+1)-J\,(J+1)-J'(J'+1)]. \tag{3.6}$$

Obviously, the spectrum of the spin–spin interaction has the chiral property since a part of it is the mirror image of the other one, with respect to zero.

Let us see what happens with the whole Hamiltonian H. It is easy to show that the following equations approximately hold

$$\begin{aligned} H\Psi^{(2qp;J1)}_{JI;M}&=[\langle\Psi^{(2qp;J1)}_{JI;M}|H_{\rm GCSM}|\Psi^{(2qp;J1)}_{JI;M}\rangle+2E_j+\lambda_{JI}]|\Psi^{(2qp;J1)}_{JI;M}\rangle,\\ HC_{12}|\Psi^{(2qp;J1)}_{JI;M}\rangle&=[\langle\Psi^{(2qp;J1)}_{JI;M}|H_{\rm GCSM}|\Psi^{(2qp;J1)}_{JI;M}\rangle+2E_j-\lambda_{JI}]C_{12}|\Psi^{(2qp;J1)}_{JI;M}\rangle. \end{aligned} \tag{3.7}$$

Therefore the Hamiltonian H also exhibits chiral features, since part of the spectrum is the mirror image of the other one, with respect to an intermediate spectrum given by averaging $H_{\rm GCSM}+\sum_\alpha E_a a^\dagger_\alpha a_\alpha$ with the function $|\Psi^{(2qp;J1)}_{JI;M}\rangle$.

Similar considerations can also be applied to the Hamiltonian H and to the pair of states $|\Psi^{(2qp;J1)}_{JI;M}\rangle$ and $C_{13}|\Psi^{(2qp;J1)}_{JI;M}\rangle$. Since the Hamiltonian transformed by C_{14} is identical to the one corresponding to the transformation $\mathbf{J_p}\to-\mathbf{J_p}$, the two transformed Hamiltonians have identical spectra.

Summarizing the above results, one can say that the spectrum of H within the restricted space $|\Psi^{(2qp;J1)}_{JI;M}\rangle$ forms a chiral band denoted, conventionally, with B_1. The eigenvalues of H obtained by averaging it with the transformed wave function $C_{12}|\Psi^{(2qp;J1)}_{JI;M}\rangle$ form the chiral partner band denoted by B_2. Another partner band of B_1 is B_3 corresponding to the chiral transformed functions $C_{13}|\Psi^{(2qp;J1)}_{JI;M}\rangle$. The partner band of B_1, denoted hereafter with B_4, obtained by averaging H with $C_{14}|\Psi^{(2qp;J1)}_{JI;M}\rangle$ is identical to B_3. Note that the symmetry generated by the transformations C_{13} and C_{14} are broken by two terms, namely the spin–spin particle–core interaction and the rotational term $2A_4\mathbf{J_p}\cdot\mathbf{J_n}$ involved in $H_{\rm GCSM}$. The latter term is ineffective in a state where the angular momenta $\mathbf{J_p}$ and $\mathbf{J_n}$ are orthogonal. Since the wave-function $|\Psi^{(2qp;J1)}_{JI;M}\rangle$ is asymmetric with respect to the proton–neutron permutation, the average values of the sS term with the transformed functions $C_{13}|\Psi^{(2qp;J1)}_{JI;M}\rangle$ and $C_{14}|\Psi^{(2qp;J1)}_{JI;M}\rangle$ are vanishing. Therefore, the degenerate bands B_3 and B_4 are essentially determined by the symmetry breaking term generated by $A_4\hat{J}^2$, i.e. $-4A_4\mathbf{J_p}\cdot\mathbf{J_n}$. Concluding, there are four chiral partner bands B_1, B_2, B_3, B_4, obtained with H and the wave functions $|\Psi^{(2qp;J1)}_{JI;M}\rangle$, $C_{12}|\Psi^{(2qp;J1)}_{JI;M}\rangle$, $C_{13}|\Psi^{(2qp;J1)}_{JI;M}\rangle$, $C_{14}|\Psi^{(2qp;J1)}_{JI;M}\rangle$, respectively.

The chiral transformation can always be written as a product of a rotation with an angle equal to π and a time reversal operator. The rotation is performed around one of the axes defined by $\mathbf{J_F}$, $\mathbf{J_p}$, $\mathbf{J_n}$ which, in the situation when they form an orthogonal set of vectors, coincide with the axes of the body fixed frame. Since the Hamiltonian has terms which are linear in the rotation generators mentioned above, it is not invariant with respect to these rotations. H is however invariant to the rotations in the laboratory frame, generated by the components of the total angular momentum, $\mathbf{J_F}+\mathbf{J_p}+\mathbf{J_n}$. The fingerprints of such an invariance can be found also in the structure of the wave functions describing the eigenstates of H in the laboratory frame. This can be easily understood by having in mind the following aspects. The proton and neutron angular momenta of the core are nearly perpendicular vectors

Table 1. The structure coefficients involved in the model Hamiltonian and described as explained in the text, are given in units of MeV. We also list the values of the deformation parameter ρ (a-dimensional) and the gyromagnetic factors of the three components, protons, neutrons and fermions, given in units of nuclear magneton (μ_N).

ρ	A_1	A_2	A_3	A_4	X_{sS}	g_p (μ_N)	g_n (μ_N)	g_F (μ_N)
1.6	1.114	−0.566	4.670	0.0165	0.0015	0.492	0.377	1.289

in a plane perpendicular to the symmetry axis, in a certain spin interval. However, we cannot distinguish between the orientation of $\mathbf{J_p}$ along the x or y axes. In the first case the intrinsic reference frame would be right-handed, while in the second one it is left-handed. In other words, the wave function must comprise one component which corresponds to the right-handed frame and one component corresponding to the left-handed frame, and, moreover, the two components should be equally probable. Their weights are then either identical or equal in magnitude but of opposite sign. Since the transformation C_{13} changes the direction of $\mathbf{J_p}$, it will change the left- to the right-handed component and vice versa. It results that the states $|\Psi^{(2qp;J1)}_{JI;M}\rangle$ are eigenstates of C_{13}. Similar reasoning is valid also for the transformation C_{12}, the component corresponding to the orientation of $\mathbf{J_F}$ along the z axis being equally probable with the component with $\mathbf{J_F}$ having an opposite direction.

5. Numerical results and discussion

The present formalism has been applied to the case of ^{138}Nd. The reason for which we chose to apply the present formalism to ^{138}Nd is that it has been proven that this nucleus is triaxial both at low and high spins, through a coherent interpretation of most of the multitude of observed bands. The triaxiality is a prerequisite of the chiral motion predicted by the present formalism. The experimental data were taken from [23, 24]. We interpreted the state of 2.273 MeV as being the state 2^+_β, since it is populated by the Gamow–Teller beta decay of the state 3^+ from ^{138}Pm [27]. Among the eight observed dipole bands in ^{138}Nd, there are two bands which could have chiral character: band $D3$ which is suggested as chiral partner of band $D2$ in [23] within the *TAC* formalism, and band $D4$ for which two possible configurations of two and four quasiparticles were suggested in [23], but which has characteristics compatible with the present GCSM formalism which predicts chiral bands of different nature. Indeed for band $D4$, both the level energies and the transition probabilities are in agreement with the present formalism. Firstly, the band-head energy of band $D4$ is the lowest among the eight observed dipole bands and is in agreement with the energy calculated by GCSM using realistic assumptions for the model parameters. Secondly, the band is composed of only dipole transitions, which is in agreement with the prediction of the present formalism. Thirdly, a possible chiral partner has been identified. All these features, which will be discussed in this section, induced us to propose band $D4$ as a candidate for the new chiral mode. The collective states from the ground, β and γ bands were described by means of the GCSM. The particle–core term is associated to the protons from $h_{11/2}$ interacting with the core through the spin–spin term.

The structure coefficients A_1, A_2, A_3, A_4 were fixed by fitting the experimental energies of the states 2^+_g, 10^+_g, 2^+_β, 2^+_γ. The deformation parameter ρ was chosen such that an overall agreement is obtained. The fitting procedure adopted provides the parameters listed in table 1. From there we notice two peculiarities, namely the attractive character of the interaction multiplying A_2 and the large magnitude of the A_3 coefficient. The first feature reflects the fact

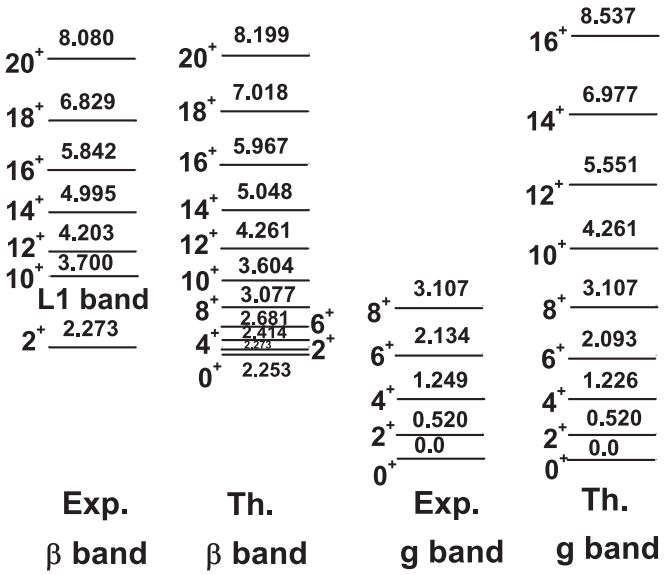

Figure 1. The calculated energies for ground and beta bands are compared with the corresponding experimental values. Also the levels from band L1 are shown since their energies are close to the calculated energies of the β band.

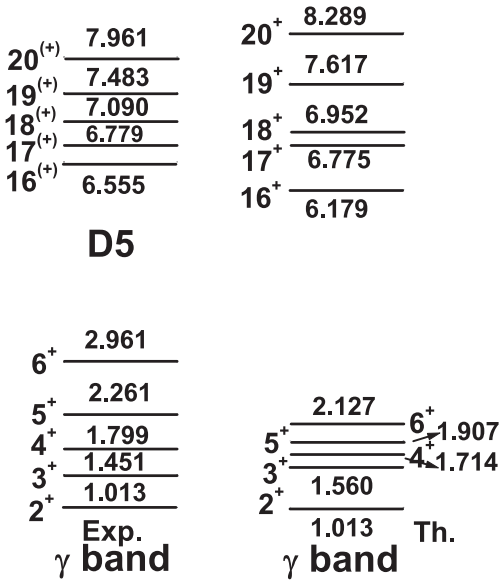

Figure 2. The theoretical values of the γ band energies are compared with the corresponding experimental data. The high spin states lie in the energy region of the experimental $D5$ band.

that the proton–neutron boson interaction, in the lowest order, tends to destabilize the boson ground state. The large value of A_3 can be understood by recalling the dependence of the band energies on the structure coefficients [12], which actually suggests the algorithm adopted for

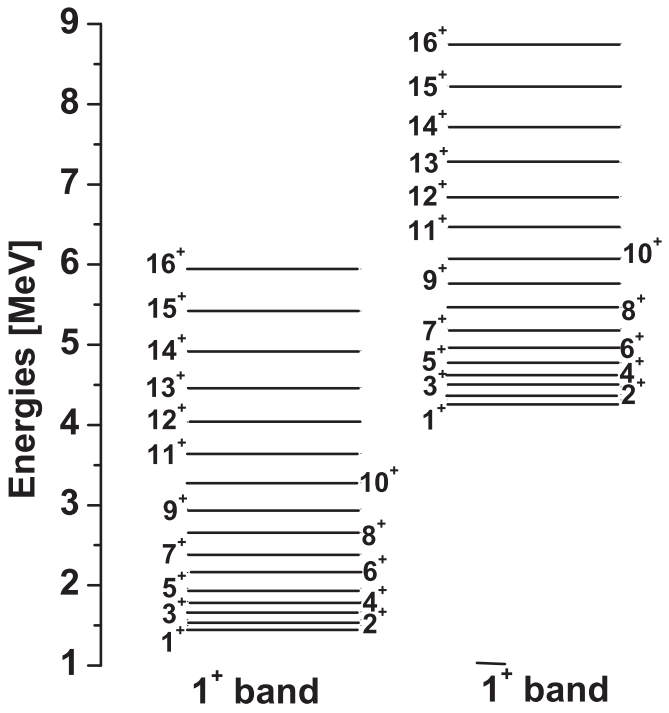

Figure 3. The calculated excitation energies for the the dipole band 1^+. Also, the energies for the dipole band $\tilde{1}^+$ are shown.

the fitting procedure. Indeed, the excitation energies in the ground band depend on $A_1 + A_2$ and A_4. Therefore these parameters are fixed by fitting two energy levels from the ground band; our choice was the energies for 2_g^+ and 10_g^+. The γ band energies are functions of $A_1 + A_2$, A_4 and $A_1 - A_2$. Thus by fitting the 2_γ^+ energy, one obtains $A_1 - A_2$. The β band energies depend, now, only on A_3. This is fixed by fitting the energy of 2_β^+. The other structure coefficients A_1, A_2 and A_4 yield too high energies for the beta band. In order to obtain a realistic description of the state 2_β^+ an important quenching is necessary, which is brought by the A_3 term. Coming back to the interaction whose strength is A_2 we notice that this is just the OX component, F_1, of the F-spin operator. In fact this is the lowest order term which violates the F-spin invariance. Thus, the eigenstates of $H_{\rm GCSM}$ are mixed F-spin states. However, the expected values of $F_0\left(=\frac{1}{2}(\hat{N}_p - \hat{N}_n)\right)$ corresponding to the projected model states are equal to zero and this is caused by the fact that the deformation parameters associated to the two kinds of bosons are equal. Note that the energies of the bands $\tilde{\gamma}$, 1^+ and $\tilde{1}^+$, are free of any adjustable parameters. As shown in figures 1 and 2, a reasonable agreement with the experimental data is obtained for the ground and β bands, while the calculated γ band is more compressed than the experiment shows.

As we already mentioned, the constraints of the GCSM formalism are satisfied by two model states for gamma and two for dipole bands: one symmetric and one asymmetric with respect to the proton–neutron permutation for gamma bands, and two asymmetric functions for dipole bands. In our calculations the symmetric states are considered for the gamma band. As for the β band, we present the energies up to the high spin region, even if the experimental data are missing. The reason for this option concerning the β band was to show that these

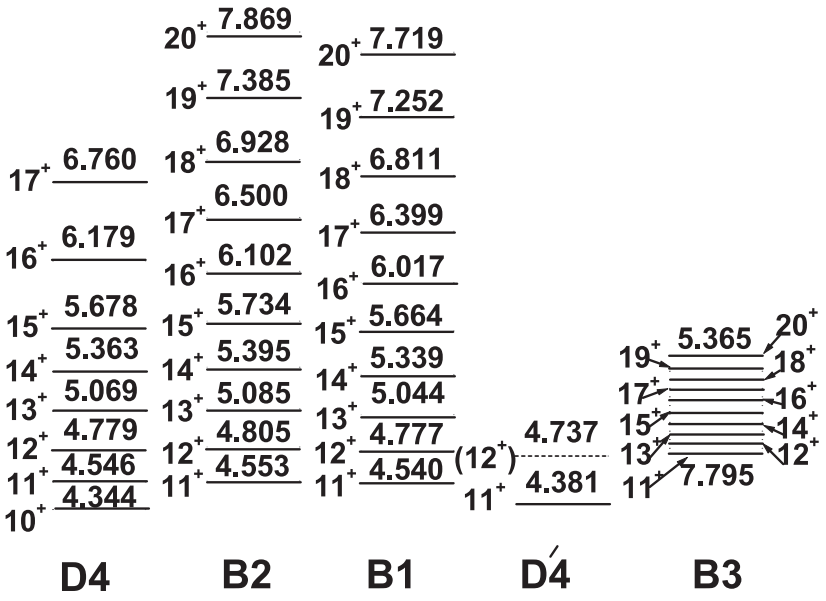

Figure 4. The excitation energies, given in MeV, for the bands B_1, B_2, B_3 and B_4. The experimental chiral partner bands $D4$ and $D'4$ are also shown. The band B_2 is to be compared with the experimental band $D4$, while B_1 with $D'4$.

energies lie close to the energy levels of band $L1$. It is an open question whether the high spin states of the β band can be assigned to band L1.

Results for the dipole bands 1^+ and $\tilde{1}^+$ are shown in figure 3.

The experimental dipole band $D4$ was not well understood in [23] in the framework of cranked Nilsson Strutinsky (CNS) and tilted axis cranking (TAC) calculations. The two proposed configurations involve either two positive-parity proton orbitals from the $(d_{5/2}, g_{7/2})$ sub-shell, the second and fourth above the Fermi level, or four orbitals—two proton and two neutron orbitals of opposite parity. These configurations are calculated by the TAC model at excitation energies relative to the yrast band $L1$ much higher than the experimental one (more than 0.5 MeV). This assignment is therefore questionable, since band $D4$ is the lowest excited dipole band with band-head spin around 10^+, for which one would expect a better agreement between experiment and theory. On the other hand, in [23] only the prolate deformed configurations were investigated, in which the particle-like proton $h^2_{11/2}$ configuration is favored. In the present calculations a hole-like proton $h^2_{11/2}$ configuration is assumed, with the quasiparticle energy equal to 1.431 MeV, which for a single-j calculation would correspond to a pairing strength $G = 0.477$ MeV.

It is remarkable that there are two experimental levels which might be considered as belonging to the partner band of $D4$, hereafter denoted as $D'4$. The state 11^+ at 4.381 MeV has been reported in [23], while the tentative (12^+) state at 4.737MeV has been identified after revisiting the same experimental data reported in [23]. The new (12^+) state is populated by a weak transition of 332 keV from the 13^+ state of band $D4$ and decays to the 11^+ state at 4.381 MeV through a 356 keV transition. As the new (12^+) state is very weakly populated, one could not assign a definite spin-parity. However, the 12^+ assignment is the most plausible, since other spin values or negative parity would led to unrealistic values of the connecting transitions. The corresponding 11^+ and 12^+ calculated levels of band B_1 have

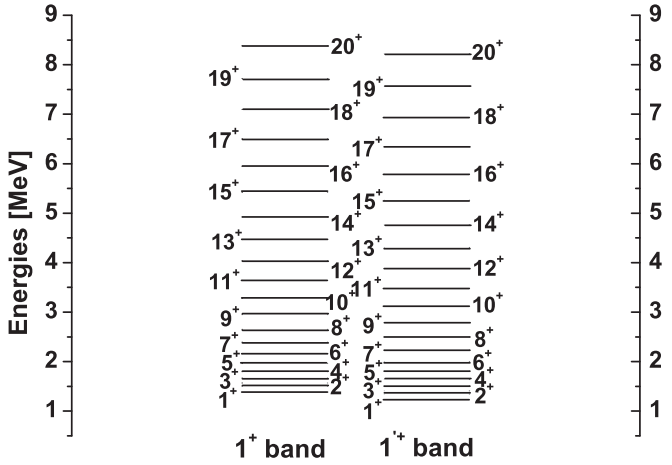

Figure 5. The excitation energies, given in MeV, for the partner bands 1^+ and $1'^+$.

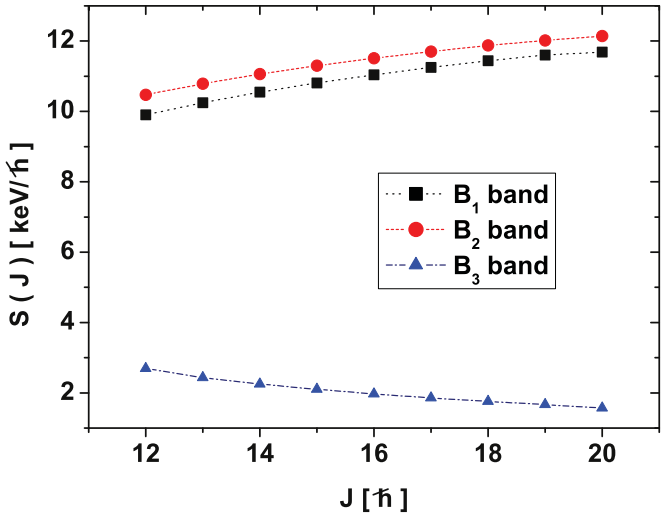

Figure 6. The energy staggering function given in units of keV$/\hbar$, is represented as function of J for the partner bands B_1 and B_2 as well as for the band B_3.

energies of 4.776 and 4.540 MeV, respectively, which are close to the experimental values of 4.737 and 4.381 MeV.

In the present paper we attempt to describe the experimental dipole band $D4$ by using the states from the basis (3.2) and the Hamiltonian (3.3).

The results are presented in figure 4. The bands B_1 and B_2 were obtained by averaging H (3.1) with the functions $|\Psi^{(2qp;J1)}_{JI;M}\rangle$, $C_{12}|\Psi^{(2qp;J1)}_{JI;M}\rangle$ respectively, while the bands B_3 and B_4 were obtained by averaging H with the functions $C_{13}|\Psi^{(2qp;J1)}_{JI;M}\rangle$ and $C_{14}|\Psi^{(2qp;J1)}_{JI;M}\rangle$, respectively. The two bands are degenerate and therefore in figure 4 we mentioned only B_3

The excellent agreement between the excitation energies of the band B_2 and the corresponding experimental ones for band $D4$ are given in the first column of figure 4. The level energy spacing of the partner bands is determined by the strength of the spin–spin

interaction, while the position of the band-head energy is determined by the pairing strength. Note that the quasiparticle energy shifts the spectrum of H by a constant value. Also, we remark that because the levels of the chiral partner bands are superpositions of states having different factor collective states, the contribution of the core to the excitation energies of the chiral band can be expressed as a sum of weighted core energies. The energy spacing in the partner band B_3 is constant (about 60 keV) with a deviation of at most 3 keV. It is very interesting to note that under the chiral transformation C_{13} the rotational term $\hat{J}_c^2$ involved in $H_{\rm GCSM}$ becomes $(J_p - J_n)^2$. This term appearing in the chiral transformed Hamiltonian is essential in determining the partner band B_3. On the other hand, we recall that such a term is used by the two-rotor model to define the scissor mode. In that respect the partner band B_3 may be interpreted as the second order scissor band. We notice that the chiral transformations C_{13} and C_{14} also affect the core's Hamiltonian $H_{\rm GCSM}$. Consequently, each collective band will have a partner band obtained by averaging $H_{\rm GCSM}$ with the corresponding chirally transformed state. To give an example, we represent the dipole partner bands 1^+ and $1'^+$ in figure 5. One expects that the two sister bands be collectively excited from the ground band. If this will be experimentally confirmed, it would be another new type of chirality. Another signature for chiral doublet bands is the behavior of the energy staggering function. This function is plotted in figure 6 for the bands B_1, B_2 and B_3. One notices that the energy staggering functions associated to the bands B_1 and B_2 are almost constant and very close to each other which, again, confirms the chiral character of the mentioned doublet.

The magnetic dipole transitions are calculated with the operator

$$\mathcal{M}_{1,m} = \sqrt{\frac{3}{4\pi}}\,(g_p J_{p,m} + g_n J_{n,m} + g_F J_{F,m}). \tag{3.8}$$

The collective proton and neutron gyromagnetic factors were calculated as explained in [7]. For the sake of completeness we also give the results here

$$\begin{pmatrix} g_p \\ g_n \end{pmatrix} = \frac{3ZR_0^2}{8\pi k_p^2}\frac{Mc^2}{(\hbar c)^2}\begin{pmatrix} A_1 + 6A_4 \\ \frac{1}{5}A_3 \end{pmatrix}. \tag{3.9}$$

Here M denotes the nucleons mass, c the light velocity, while A_1, A_3, A_4 are the structure coefficients involved in the phenomenological GCSM Hamiltonian. The gyromagnetic factors depend also on the parameter k_p which relates the proton–quadrupole coordinates and the proton–boson operators. This has been analytically expressed in [8] with the result

$$k_p^2 = \frac{3}{16\pi}AR_0^2\frac{Mc^2}{(\hbar c)^2}\left(A_1 + 6A_4 + \frac{1}{5}A_3\right). \tag{3.10}$$

The results for the collective gyromagnetic factors are those shown in table 1. The fermionic gyromagnetic factor is that characterizing two protons in the shell $h_{11/2}$ with a quenching factor for the neutron spin factor of about 0.75.

The magnetic dipole reduced transition probabilities within each of the four chiral bands are listed in table 2, as function of the final state angular momentum. Note that although the B (M1) values in the four chiral bands have similar behavior as the function of the angular momentum, they substantially differ quantitatively from each other. The large magnitude of these transitions within the band B_2 is remarkable, where the angular momentum of the fermions is oriented differently than that in band B_1. It signifies that changing the sign of one gyromagnetic factor favors the increase of the $B(M1)$ values. We also notice that although the bands $B3$ and $B4$ are degenerate, the associated B(M1) values are different. Concluding, the

Table 2. The magnetic dipole proton–neutron and fermion transition amplitudes for the bands B_1, B_2, B_3, B_4.

	B_1 band			B_2 band			B_3 band			B_4 band		
I	B(M1)	$A_{pn}^{(I)}$	$A_F^{(I)}$	B(M1)	$A_{pn}^{(I)}$	$A_F^{(I)}$	$B(M1)$	$A_{pn}^{(I)}$	$A_F^{(I)}$	$B(M1)$	$A_{pn}^{(I)}$	$A_F^{(I)}$
11^+	0.662	−1.041	2.705	3.352	−1.041	-2.705	1.931	0.138	2.705	1.574	−0.138	2.705
12^+	1.664	−0.989	3.629	5.093	−0.989	-3.629	3.376	0.131	3.629	2.922	−0.131	3.629
13^+	2.596	−0.933	4.231	6.365	−0.933	-4.231	4.526	0.123	4.231	4.027	−0.123	4.231
14^+	3.409	−0.886	4.665	7.358	−0.886	-4.665	5.460	0.117	4.665	4.938	−0.117	4.665
15^+	4.109	−0.847	4.996	8.151	−0.847	-4.996	6.229	0.112	4.996	5.694	−0.112	4.996
16^+	4.711	−0.813	5.256	8.796	−0.813	-5.256	6.868	0.108	5.256	6.328	−0.108	5.256
17^+	5.231	−0.784	5.465	9.325	−0.784	-5.465	7.405	0.104	5.465	6.863	−0.104	5.465
18^+	5.681	−0.758	5.637	9.762	−0.758	-5.637	7.857	0.100	5.637	7.317	−0.100	5.637
19^+	6.071	−0.734	5.777	10.123	−0.734	-5.777	8.239	0.097	5.777	7.702	−0.097	5.777

Table 3. The calculated reduced probabilities for the E2 transitions $I \to (I-2)$, $I \to (I-1)$ and $I \to I$, given in units of $[e^2b^2]$.

I	$I \to (I-2)$	$I \to (I-1)$	$I \to I$
11			0.3083
12		0.0477	0.1771
13	0.0015	0.1068	0.0994
14	0.0096	0.1380	0.0533
15	0.0232	0.1533	0.0264
16	0.0376	0.1578	0.0112
17	0.0544	0.1579	0.0035
18	0.0587	0.1538	0.0004
19	0.0858	0.1490	0.0002
20	0.0985	0.1421	0.0019

dependence of the magnetic dipole transition intensities on the nature of the chiral band is a specific feature of the present formalism.

The effect of the chiral transformation on the $B(M1)$ values can be understood by analyzing the relative signs of the collective and fermionic transition amplitudes. Indeed, the reduced transition probability can be written as

$$B(M1; I+1 \to I) = \frac{3}{4\pi}(A_{pn}^{(I)} + A_F^{(I)})^2, \tag{3.11}$$

where $A_{pn}^{(I)}$ denotes the terms of the transition matrix elements which are linear combination of the gyromagnetic factors g_p and g_n, while $A_F^{(I)}$ is that part which is proportional to g_F. Their values for the transitions in the four chiral bands are listed in table 2.

Note that for the bands B_2 and B_3 the contributions of the collective and fermion transition amplitudes are in phase, while for the other bands they exhibit different phases. This explains the large magnitude of the transitions in the bands B_2 and B_3 compared with those within the bands B_1 and B_4. In fact, such behavior is proof that by a chiral transformation the transversal magnetic moment is increased. The intra-band transitions for the doublet bands B_1 and B_2, suspected to be of chiral nature, vary monotonically in the intervals $0.66 - 6.07\mu_N^2$ and $3.4 - 10.12\mu_N^2$, respectively.

The quadrupole electric transition probabilities were calculated using for the transition operator the expression

$$\mathcal{M}_{2\mu} = \frac{3ZeR_0^2}{4\pi}\alpha_{p\mu}, \tag{3.12}$$

where the quadrupole collective coordinate, $\alpha_{p\mu}$, is related with the corresponding boson operators by the canonical transformation

$$\alpha_{p\mu} = \frac{1}{\sqrt{2}\,k_p}(b_{p\mu} + (-)^{\mu}b_{p,-\mu}). \tag{3.13}$$

The standard notations for the nuclear charge, electron charge and nuclear radius are used. The above transformation is canonical irrespective the value of k_p, which is determined as described in [8], with the result mentioned above.

Since the quadrupole transition operator is invariant to any chiral transformation, the $B(E2)$ values for the intra-band transitions in the four chiral bands are the same. The common values are given in table 3. One notices the small $B(E2)$ reduced transition probabilities,

compared with the transitions in the well deformed nuclei, for the intra-band transitions which, in fact, is a specific feature of the chiral bands. Note that the $B(E2; I \to (I-1))$ values increase with I at low spins and decrease with I at high spins. Note that the stretched and crossover transitions are very small, almost vanishing.

6. Conclusions

In the previous sections we described a particle–core formalism for the chiral bands. The application is made for ^{138}Nd, where some experimental data are available [23, 24]. The phenomenological core is described by the GCSM. Particles move in a spherical shell model mean-field and alike nucleons interact among themselves through pairing. The outer particles interact with the core by a spin–spin force. The model Hamiltonian was treated within a restricted space associated to the phenomenological core and the subspace of aligned two proton quasiparticle states, from the $h_{11/2}$ sub-shell, coupled to the states of the phenomenological scissor-like dipole states.

The eigenvalues of the model Hamiltonian within the particle–core subspace are arranged in four bands denoted by B_1, B_2, B_3 and B_4, respectively. The bands B_3 and B_4 correspond to the particle–core states transformed by changing $\mathbf{J_p} \to -\mathbf{J_p}$ and $\mathbf{J_n} \to -\mathbf{J_n}$ respectively and are degenerate. Energies as well as the $M1$ and the $E2$ transition rates for these bands are quantitatively studied. The results of our calculations confer the character of chiral doublet partners to the bands B_1 and B_2.

Also, the intra-band $B(M1)$ values are large and vary when one passes from one band to another. In contrast, the $B(E2)$ values do not depend on the band and in general are small. The energy spacing in all four bands is almost constant. This is reflected by the associated energy staggering functions shown in figure 6. As a matter of fact these properties confer the bands B_1 and B_2 a chiral character. The bands B_2 and B_1 describe the experimental bands $D4$ and $D'4$ of ^{138}Nd.

Our work proves that the mechanism for chiral symmetry breaking, proposed in [5], which also favors a large transverse component for the dipole magnetic transition operator, is not unique.

Note that the bands B_3, B_4, as well as the partner bands associated to the collective bands describing the core, emerge from their sister bands by considering the contribution of the collective term $(\mathbf{J_p} - \mathbf{J_n})^2$. Recalling that such a term determines the excitation energy of the scissor mode, we can call the mentioned doublet members second order scissor bands.

In order to compare the present approach to the existing formalisms, we have to remember few specific features of the preceding procedures. For odd–odd nuclei several groups identified twin bands in medium mass regions [26–31] and even in heavy mass regions [32–34]. The formalisms proposed for these bands were based either on the tilted axis cranking (TAC) approach [35] or on the two quasiparticle-triaxial rotor coupling model [36–39]. Although the efforts were mainly focused on identifying and describing the chiral twin bands in odd–odd nuclei, a few results for even–odd [40–45] and even–even [46] nuclei were also reported.

Also, it is worth mentioning another boson description of the chiral phenomenon, which uses the interacting boson–fermion–fermion model (IBFFM-1) [47–50]. This hinges on the interacting boson model (IBM-1) (where there is no distinction between proton bosons and neutron bosons) for even–even nuclei and IBFM-1 for odd–A nuclei. The vibrational and rotational degrees of freedom are taken into account in describing the core by the interacting boson model (IBM) with O(6) dynamical symmetry which resulted in proposing a dynamic

chirality with the shape fluctuation [48]. Within the IBFFM-1, a triaxial shape is obtained by adding to the IBM1 Hamiltonian, describing the even–even core, a cubic (three-body) term. Also, it was shown that an important improvement of the agreement between the calculated and corresponding experimental data in the odd–A nuclei is obtained if the exchange effect is accounted for. This effect reflects the anti-symmetrization of the odd nucleon and the nucleons involved in the boson structure. Within the IBFFM-1 [49] the dynamic chirality in ^{134}Pr was also studied. The analysis of the wave functions has shown that the possibility for angular momenta of the valence proton, neutron and core to find themselves in the favorable, almost orthogonal geometry, is present but not dominant. Such behavior is found to be similar in nuclei where both the level energies and the electromagnetic decay properties display the chiral pattern, as well as in those where only the level energies of the corresponding levels in the twin bands are close to each other. The difference in the structure of the two types of chiral candidates nuclei can be attributed to different β and γ fluctuations, induced by the exchange boson–fermion interaction of the interacting boson fermion–fermion model, i.e. the anti-symmetrization of odd fermions with the fermion structure of the bosons. In both cases the chirality is weak and dynamic. The interacting boson–fermion model was extended by including broken proton and broken neutron pairs [51]. The application to ^{136}Nd showed a very good agreement with experimental data for eight dipole bands, including the high spin region.

The formalism proposed in the present paper concerns the even–even nuclei and is based on a new concept. Indeed, there are few features which are different from the main characteristics of the model proposed by Frauendorf for odd–odd nuclei [5, 35]. Indeed, here the right- and left-handed frames are the angular momentum carried by two aligned protons and by proton and neutron bosons respectively, associated to the core. Within the model proposed by Frauendorf, the shear motion is achieved by one proton–particle and one neutron–hole, while here the shear blades are the proton and neutron components of the core. The $B(M1)$ values are maximal, in Frauendorf's model, at the beginning of the band and decrease with angular momentum and finally, when the shears are closed, they are vanishing since there is no longer any transverse magnetic momentum. By contrast, in the present formalism the $B(M1)$ values increase with the angular momentum. In both models the dominant contribution to the dipole magnetic transition probability is coming from the particle sub-system. This property is determined by the specific magnitudes of the gyromagnetic factors associated to the three components of the system. Due to the fact that only a few particles participate in determining the quantitative properties, the chiral bands seem to be of a non-collective nature. Since the two schematic models reveal some complementary magnetic properties of nuclei, they might cover different areas of nuclear spectra.

Acknowledgments

This work was supported by the Romanian Ministry for Education, Research, Youth and Sport through the CNCSIS project ID-2/5.10.2011.

References

[1] Iudice N L and Palumbo F 1978 *Phys. Rev. Lett.* **41** 1532
[2] De Francheschi G, Palumbo F and Iudice N L 1984 *Phys. Rev.* C **29** 1496
[3] Iudice N L 1997 *Phys. Part. Nucl.* **25** 556
[4] Zawischa D 1998 *J. Phys. G: Nucl. Part. Phys.* **24** 683
[5] Frauendorf S 2001 *Rev. Mod. Phys.* **73** 463

[6] Jenkins D G *et al* 1999 *Phys. Rev. Lett.* **83** 500
[7] Raduta A A, Raduta C M and Faessler A 2014 *J. Phys. G: Nucl. Part. Phys.* **41** 035105
[8] Raduta A A and Raduta C M 2015 *J. Phys. GL Nucl. Part. Phys.* **42** 065105
[9] Raduta A A and Budaca R 2014 *Ann. Phys. (NY)* **347** 141
[10] Liang Y, Ma R, Paul E S, Xu N, Fossan D B, Zhang J Y and Donau F 1990 *Phys. Rev. Lett.* **64** 29
[11] Paul E S, Fossan D B, Liang Y, Ma R, Xu N, Wadsworth R, Jenkins I and Nolan P J 1990 *Phys. Rev.* C **41** 1576
[12] Raduta A A, Faessler A and Ceausescu V 1987 *Phys. Rev.* C **36** 439
[13] Raduta A A *et al* 1981 *Phys. Lett.* B **121** 1
Raduta A A *et al* 1982 *Nucl. Phys.* A **381** 253
[14] Sheline R K 1960 *Rev. Mod. Phys.* **32** 1
Sakai M 1976 *Nucl. Phys.* A **104** 301
[15] Raduta A A, Ursu I I and Delion D S 1987 *Nucl. Phys.* A **475** 439
[16] Raduta A A and Delion D S 1989 *Nucl. Phys.* A **491** 24
[17] Iudice N L *et al* 1993 *Phys. Lett.* B **300** 195
Iudice N L *et al* 1994 *Phys. Rev.* C **50** 127
[18] Raduta A A, Lima C and Faessler A 1983 *Z. Phys. A—Atoms and Nuclei* **313** 69
[19] Iudice N L *et al* 1993 *Phys. Lett.* B **300** 195
Iudice N L *et al* 1994 *Phys. Rev.* C **50** 127
[20] Lo Iudice N, Raduta A A and Delion D S 1994 *Phys. Rev.* C **50** 127
[21] Maruhn-Rezwani V, Greiner W and Maruhn J A 1975 *Phys. Lett.* B **57** 109
[22] Novoselski A and Talmi I 1985 *Phys. Lett.* B **60** 13
[23] Petrache C M *et al* 2012 *Phys. Rev.* C **86** 044321
[24] Li H J *et al* 2013 *Phys. Rev.* C **87** 057303
[25] Raduta A A 2015 *Nuclear Structure with Coherent States* (Cham: Springer)
[26] Grodner E 2008 *Acta Phys. Pol.* B **39** 531
[27] Deslauriers J, Gujrathi S C and Mark S K 1981 *Z. Phys.* A **303** 151
[28] Petrache C M *et al* 1996 *Nucl. Phys.* A **597** 106
[29] Simon A J *et al* 2005 *Jour. Phys. G: Nucl. Part. Phys.* **31** 541
[30] Vaman C *et al* 2004 *Phys. Rev. Lett.* **92** 032501
[31] Petrache C M *et al* 2006 *Phys. Rev. Lett.* **96** 112502
[32] Balabanski D L *et al* 2004 *Phys. Rev.* C **70** 044305
[33] Frauendorf S and Meng J 1997 *Nucl. Phys.* A **617** 131
[34] Dimitrov V I, Frauendorf S and Donau F 2000 *Phys. Rev. Lett.* **84** 5732
[35] Frauendorf S 2000 *Nucl. Phys.* A **677** 115
[36] Toki H and Faessler A 1975 *Nucl. Phys.* A **253** 231
[37] Toki H and Faessler A 1976 *Z. Phys.* A **276** 35
[38] Toki H and Faessler A 1976 *Phys. Lett.* B **63** 121
[39] Toki H, Yadav H L and Faessler A 1977 *Phys. Lett.* B **66** 310
[40] Zhu S *et al* 2003 *Phys. Rev. Lett.* **91** 132501
[41] Alcantara-Nunez J A *et al* 2004 *Phys. Rev.* C **69** 024317
[42] Timar J *et al* 2004 *Phys. Lett.* B **598** 178
[43] Timar J *et al* 2006 *Phys. Rev.* C **73** 011301(R)
[44] Luo Y X *et al* 2009 *Chin. Phys. Lett.* B **26** 082301
[45] Ayangeakaa A D *et al* 2013 *Phys. Rev. Lett.* **110** 172504
[46] Mergel E *et al* 2002 *Eur. Phys. J.* A **15** 417
[47] Tonev D *et al* 2006 *Phys. Rev. Lett.* **96** 052501
[48] Tonev D *et al* 2007 *Phys. Rev.* C **76** 044313
[49] Brant S, Tonev D, de Angelis G and Ventura A 2008 *Phys. Rev.* C **78** 0343301
[50] Brant S and Petrache C M 2009 *Phys. Rev.* C **79** 054326
[51] Vretenar D *et al* 1998 *Phys. Rev.* C **57** 675